Molecular Cell

Article

The HRI branch of the integrated stress response selectively triggers mitophagy

Graphical abstract

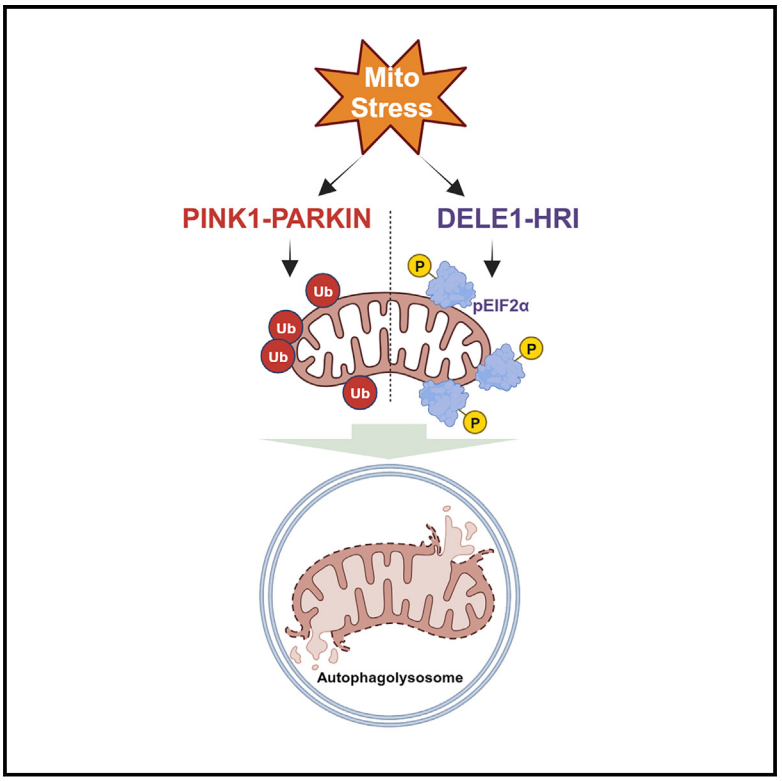

Highlights

- Heme-regulated inhibitor branch of the integrated stress response drives mitophagy
- Mitochondrial localization of phospho-EIF2α is crucial for mitophagy induction
- Several types of mitophagy, including PINK1/PARKIN, are regulated by HRI
- HRI and PINK1/PARKIN are parallel pathways for mitophagy with distinct mechanisms

Authors

Yogaditya Chakrabarty, Zheng Yang, Hsiuchen Chen, David C. Chan

Correspondence

dchan@caltech.edu

In brief

Mitochondrial quality control depends on regulating mitochondrial turnover in response to cellular stress. Chakrabarty et al. show that the heme-regulated inhibitor branch of the integrated stress response, in response to mitochondrial stress, activates mitophagy via the mitochondrial localization of phosphorylated EIF2α, which normally functions in translational initiation.

Chakrabarty et al., 2024, Molecular Cell *84*, 1–11
March 21, 2024
https://doi.org/10.1016/j.molcel.2024.01.016

CellPress

Please cite this article in press as: Chakrabarty et al., The HRI branch of the integrated stress response selectively triggers mitophagy, Molecular Cell (2024), https://doi.org/10.1016/j.molcel.2024.01.016

Molecular Cell

CellPress

Article

The HRI branch of the integrated stress response selectively triggers mitophagy

Yogaditya Chakrabarty,[1] Zheng Yang,[1] Hsiuchen Chen,[1] and David C. Chan[1,2,*]
[1]Division of Biology and Biological Engineering, California Institute of Technology, Pasadena, CA 91125, USA
[2]Lead contact
*Correspondence: dchan@caltech.edu
https://doi.org/10.1016/j.molcel.2024.01.016

SUMMARY

To maintain mitochondrial homeostasis, damaged or excessive mitochondria are culled in coordination with the physiological state of the cell. The integrated stress response (ISR) is a signaling network that recognizes diverse cellular stresses, including mitochondrial dysfunction. Because the four ISR branches converge to common outputs, it is unclear whether mitochondrial stress detected by this network can regulate mitophagy, the autophagic degradation of mitochondria. Using a whole-genome screen, we show that the heme-regulated inhibitor (HRI) branch of the ISR selectively induces mitophagy. Activation of the HRI branch results in mitochondrial localization of phosphorylated eukaryotic initiation factor 2, which we show is sufficient to induce mitophagy. The HRI mitophagy pathway operates in parallel with the mitophagy pathway controlled by the Parkinson's disease related genes *PINK1* and *PARKIN* and is mechanistically distinct. Therefore, HRI repurposes machinery that is normally used for translational initiation to trigger mitophagy in response to mitochondrial damage.

INTRODUCTION

To maintain mitochondrial homeostasis, mitochondrial number and quality must be monitored and regulated in cells. Mitophagy is an autophagic process whereby excessive or damaged mitochondria are degraded by hydrolases within the acidic environment of the lysosome.[1,2] The importance of this process is indicated by the finding that two genes mutated in inherited forms of Parkinson's disease, PTEN-induced putative kinase protein 1 (*PINK1*) and *PARKIN* (Parkinson's disease protein 2 [*PARK2*]), function together in a key mitophagy pathway.[1,3] It has been suggested that the neurodegeneration of Parkinson's disease results from failure of mitochondrial quality control. For mitophagy to safeguard mitochondrial quality, the sensing of mitochondrial dysfunction should be linked to the induction of mitophagy. Much progress has been made identifying components mediating mitophagy, but less is known about how cell surveillance systems intersect with mitophagy.

To understand the mechanisms regulating mitochondrial homeostasis, we performed a whole-genome screen to identify factors regulating mitophagy induced by the iron chelator deferiprone (DFP). This screen unexpectedly identified multiple components of the integrated stress response (ISR), specifically those in the heme-regulated inhibitor (HRI) branch. The ISR is a conserved, cell surveillance system with four branches that respond to distinct cellular stresses.[4] Upon sensing stress, each branch has a central kinase that inhibits eukaryotic initiation factor 2 (EIF2) by phosphorylating its α subunit. The resulting reduction in EIF2 activity mediates two outputs: reduction of global protein translation and enhanced expression of select stress proteins. EIF2 is a GTP-binding protein that is a heterotrimeric complex of subunits α, β, and γ. During initiation of mRNA translation, EIF2 in its GTP-bound state recruits the initiator Met-tRNAi to the 40S ribosome. At the end of this process, the GTP is hydrolyzed, and the released EIF2-GDP complex must be reactivated by initiation factor eukaryotic translation initiation factor 2 subunit beta (EIF2B), which functions as a guanine nucleotide exchange factor (GEF) for EIF2. Phosphorylation of the α subunit of EIF2 by the ISR kinases causes EIF2 to change from a substrate to a competitive inhibitor of EIF2B. Phosphorylated EIF2 (p-EIF2) binds strongly to EIF2B, thereby sequestering the latter in an inhibited complex. The HRI and general control non-derepressible 2 (GCN2) branches of the ISR are known to sense mitochondrial dysfunction,[5–7] but it is unknown whether this detection is coupled to mitochondrial turnover.

Using a CRISPRi screen, we found that the HRI branch of the ISR plays a critical role in regulating mitochondrial quality control. Our analysis indicates that DFP activates the HRI branch to promote mitophagy. HRI activation results in accumulation of p-EIF2 on mitochondria, and we show that this localization is sufficient to trigger mitophagy. Although we identified the role of HRI in DFP-induced mitophagy, the HRI pathway is an important component in other forms of mitophagy, including PINK1/PARKIN-mediated mitophagy and hypoxia-induced mitophagy.

Please cite this article in press as: Chakrabarty et al., The HRI branch of the integrated stress response selectively triggers mitophagy, Molecular Cell (2024), https://doi.org/10.1016/j.molcel.2024.01.016

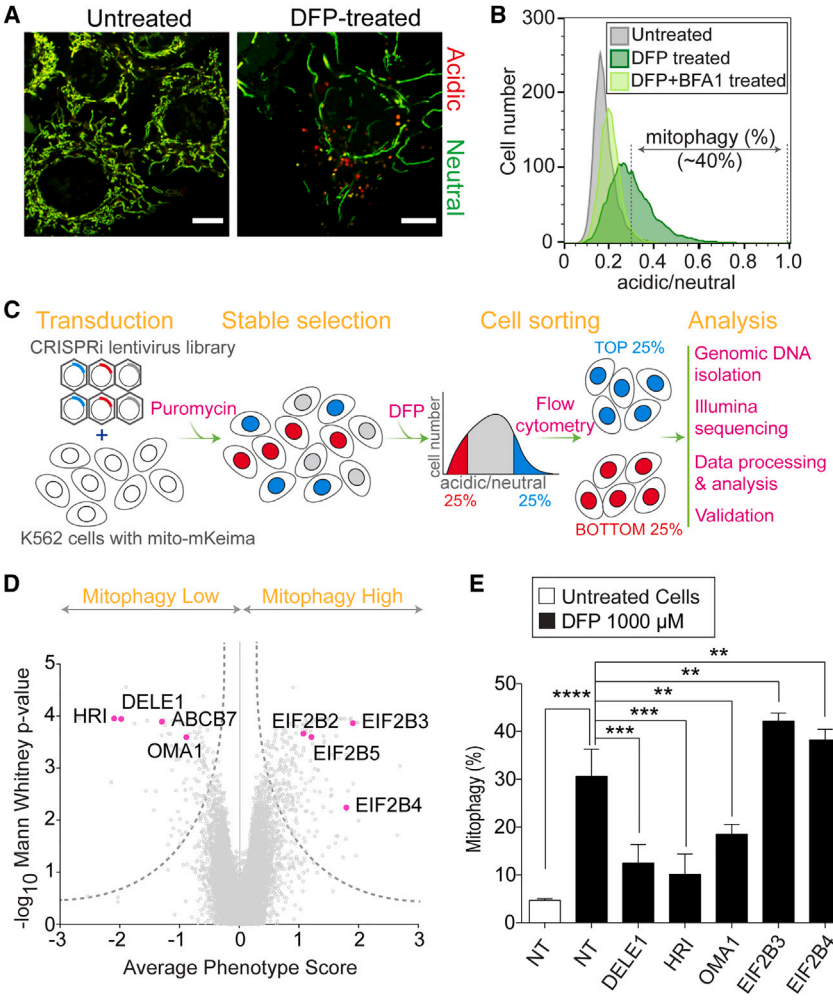

Figure 1. CRISPRi screen identifies HRI components as mitophagy factors

(A) Visualization of mitophagy with mito-mKeima. Ratiometric imaging was used to detect mitochondria in acidic compartments in HeLa cells expressing mito-mKeima. Red mitochondria have a high acidic/neutral ratio. Scale bars, 10 μm.

(B) Quantification of mitophagy in mito-mKeima-expressing K562 cells by analysis of the mKeima acidic/neutral ratio with flow cytometry. Bafilomycin A1 (BFA1) was used to block mitophagy.

(C) Workflow of the CRISPRi screen. Cells harboring the CRISPRi library were treated with DFP to induce mitophagy, and cells showing the 25% lowest and highest levels of mitophagy were collected for sgRNA analysis by deep sequencing.

(D) Volcano plot of sgRNAs from mitophagy screen. For each sgRNA, the phenotype effect size is plotted on the x axis and the p value on the y axis. The dotted line indicates the threshold for hits based on an integrated score for effect size and p value.[9] Hits of interest are highlighted in magenta and labeled.

(E) Confirmation of hits from mitophagy screen. Flow cytometry of mito-mKeima was used to quantify DFP-induced mitophagy after expression of sgRNA against indicated genes (NT, non-targeting; mean ± SD, $n \geq 4$). The following p value designations are used in all figures: ****$p \leq 0.0001$; ***$p \leq 0.001$; **$p \leq 0.01$; *$p \leq 0.05$; ns, $p \geq 0.05$.

See also Figure S1 and Table S1.

RESULTS

The ISR is essential for DFP-induced mitophagy

The iron chelator DFP strongly induces mitophagy independently of the *PINK1*/*PARKIN* pathway.[8] We used a CRISPRi library screen[9–11] to systematically identify factors required for DFP-mediated mitophagy. K562 cells were engineered to express mito-mKeima, a mitophagy reporter residing in the mitochondrial matrix.[12,13] mKeima is a pH-sensitive fluorophore displaying a bimodal excitation spectrum, with excitation at the 440 nm peak predominant above pH 6 and excitation at the 586 nm peak predominant below pH 5, as in the lysosome (Figure S1A). Induction of mitophagy was readily detected in mito-mKeima expressing cells after DFP treatment, by both fluorescence microscopy and flow cytometry (Figures 1A and 1B). As expected, bafilomycin A1 (BFA1), an inhibitor of the H+-ATPase, blocked mitophagy (Figure 1B). With flow cytometry, mitophagy could be quantified at the single-cell level by dual excitation, ratiometric imaging of mito-mKeima.[12,13] DFP caused a dose-dependent increase in cells with a high acidic/neutral ratio, rising to ~40% mitophagy at 1 mM DFP (Figure S1B). This mitophagy was indeed triggered by loss of iron availability because it was abrogated by addition of haemin, a porphyrin that coordinates Fe^{3+} (Figure S1C).

After transduction of the CRISPRi single guide RNA (sgRNA) library, DFP-treated cells containing the bottom and top 25% mitophagy levels were isolated by fluorescence-activated cell sorting (FACS), and the sgRNAs in those two populations were quantified by deep sequencing to identify genes potentially acting as positive and negative regulators of mitophagy, respectively (Figure 1C). Notably, the bottom population showed enrichment of sgRNAs for several components of the ISR pathway,[4,14] including *HRI* (also called *EIF2AK1*, eukaryotic translation initiator factor 2 alpha kinase), DAP3-binding cell death enhancer 1 (*DELE1*), overlapping with the m-AAA protease 1 homolog (*OMA1*), and ATP-binding cassette sub-family B member 7 (*ABCB7*, mitochondrial) (Figure 1D; Table S1). Previous studies showed that mitochondrial stress causes the mitochondrial metalloprotease OMA1 to cleave the intermembrane space protein DELE1, generating a short fragment (S-DELE1) that is released from mitochondria to activate the HRI kinase (Figure 2A).[6,7] HRI phosphorylates the EIF2α subunit of the trimeric translation initiation factor EIF2. p-EIF2 promotes the ISR, causing downregulation of general protein translation and upregulation of transcriptional regulators like activating transcription factor 4 (ATF4), activating transcription factor 3 (ATF3), and CCAAT/enhancer-binding protein (CHOP; also known as DNA damage-inducible transcript 3 [DDIT3]) to induce

Please cite this article in press as: Chakrabarty et al., The HRI branch of the integrated stress response selectively triggers mitophagy, Molecular Cell (2024), https://doi.org/10.1016/j.molcel.2024.01.016

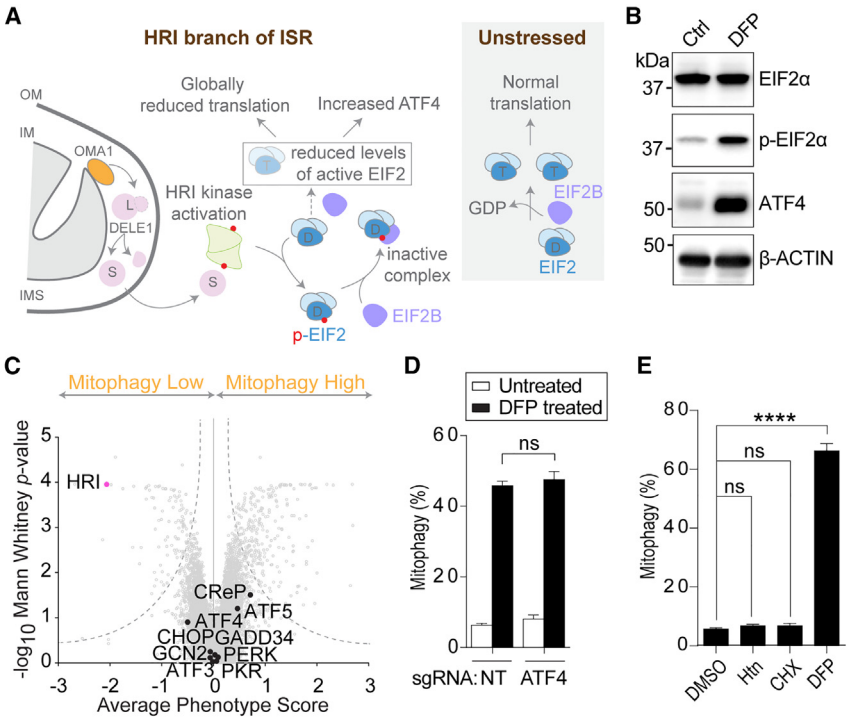

Figure 2. Iron chelation induces HRI, but mitophagy does not require ATF4

(A) A cartoon depicting the HRI branch of the ISR. Upon mitochondrial stress, the OMA1 metalloprotease cleaves DELE1 to generate a cleaved fragment (S) that is released from mitochondria and activates the kinase activity of HRI. HRI phosphorylates EIF2α and causes EIF2 to form an inhibited complex with its guanine nucleotide exchange factor EIF2B. Due to this depletion of EIF2B activity, EIF2-GDP (labeled "D") cannot be converted to its active GTP-bound state (labeled "T").

(B) Induction of ISR by DFP. Control K562 cells and DFP-treated cells were analyzed by western blotting for the indicated proteins. β-ACTIN is the loading control.

(C) Volcano plot of the genome-wide CRISPRi screen indicating HRI (magenta) versus other key factors (black) of the ISR.

(D) Effect of ATF4 knockdown on DFP-induced mitophagy. After addition DFP for 24 h, mitophagy was measured by flow cytometry in K562 cells (mean ± SD, n = 3).

(E) Effect of translation inhibitors harringtonine (Htn) and cycloheximide (CHX) on mitophagy.

See also Figure S2 and Table S1.

a stress response (Figure 2A).[4,14] ABCB7 is a mitochondrial iron exporter required for DELE1 activation during iron chelation.[15]

Further supporting a role of the ISR, the population containing high mitophagy showed enrichment of sgRNAs for several subunits of the decameric EIF2B complex (Figure 1D; Table S1). As a guanine nucleotide binding protein, EIF2 activity is dependent on EIF2B, which functions as its GEF to convert EIF2-GDP to the form active for translation, EIF2-GTP.[4,14] The p-EIF2 is a potent competitive inhibitor of EIF2B, and therefore ISR induction inhibits EIF2 activity. Because EIF2B is required for activation of EIF2 and forms a stable, inhibited complex with p-EIF2,[16–18] loss of EIF2B would prevent cycling of EIF2 into its active, GTP-bound state and also result in higher levels of uncomplexed p-EIF2. Using individual sgRNA knockdowns, we directly confirmed that the CRISPRi hits within HRI pathway are true positives. Loss of HRI, DELE1, or OMA1 reduced DFP-induced mitophagy levels, as measured by flow cytometry of mito-mKeima, whereas loss of the EIF2B subunits EIF2B3 or EIF2B4 resulted in elevated mitophagy (Figures 1E and S1D–S1F). In addition to the mito-mKeima assay, we monitored the levels of the mitochondrial inner membrane protein TIMM50 (translocase of inner mitochondrial membrane 50) as another measure of mitophagy. Western blot analysis of TIMM50 confirmed that DFP reduced mitochondrial content, and this effect was reversed by HRI, DELE1, and OMA1 knockdown (Figures S1G and S1H).

Besides the HRI pathway, our screen identified HIF1α as important for DFP-induced mitophagy, consistent with a previous report (Figure S1I).[19] Other hits previously implicated in mitophagy include TOM22 (translocase of outer mitochondrial membrane 22) and RAB7A (Ras-related protein Rab-7a).[20,21] We did not identify any known mitophagy receptors, likely because such receptors are known to have redundant functions.[22] Knockdown of respiratory chain components (e.g., NDUFS4 and UQCRB) or other critical mitochondrial proteins (e.g., POLRMT) caused increased mitophagy, likely because the knockdowns increase mitochondrial dysfunction (Figure S1I).

The HRI branch selectively triggers mitophagy

Given that knockdown of ISR components blocked DFP-induced mitophagy, we reasoned that DFP treatment likely activated the ISR. Consistent with this idea, a recent report showed activation of HRI by iron chelation in HEK293 and HeLa cells.[15] We found that mitophagy induction by DFP was associated with accumulation of both p-EIF2α and ATF4, two signatures of the ISR (Figure 2B). Knockdown of either DELE1 or HRI blocked this upregulation of ATF4 (Figure S2A).

ISR induction by phosphorylation of EIF2α results in global reduction of translation initiation and activation of select transcriptional programs by upregulation of ATF4 (Figure 2A).[4,14] However, our CRISPRi screen did not show an effect for ATF4 or other ISR upregulated genes such as ATF3, CHOP, and GADD34 (growth arrest and DNA damage inducible 34; also known as protein phosphatase 1 regulatory subunit 15A [PPP1R15A]) (Figure 2C). Consistent with this result, we found that knockdown of ATF4 in K562 cells by sgRNA was ineffective at preventing DFP-mediated mitophagy (Figures 2D and S2B). We obtained similar results in HeLa cells. Knockdown of DELE1, OMA1, and HRI suppressed DFP-induced mitophagy, whereas knockdown of ATF4 did not (Figures S2C–S2G).

Because ATF4 is not required for HRI-mediated mitophagy, we tested the role of reduced translation levels. Cycloheximide (CHX) has been used in previous reports to mimic ISR-induced translation reduction.[7,23] Treatment of K562 cells with different

Please cite this article in press as: Chakrabarty et al., The HRI branch of the integrated stress response selectively triggers mitophagy, Molecular Cell (2024), https://doi.org/10.1016/j.molcel.2024.01.016

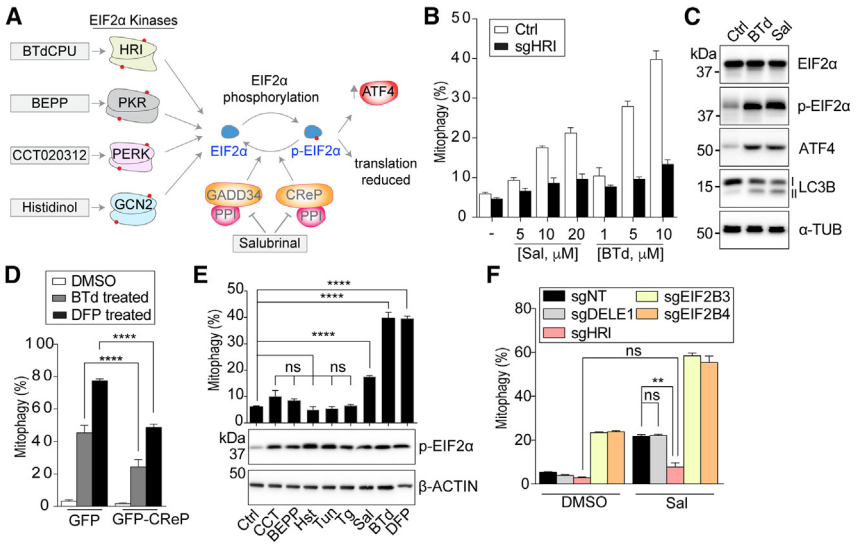

Figure 3. HRI is the only ISR branch that triggers mitophagy

(A) A schematic of the chemical reagents (rectangles on left) activating the four branches of the ISR. Each branch contains a key kinase that phosphorylates EIF2α to suppress global translation and activate ATF4 translation. Salubrinal can also increase p-EIF2α by inhibiting phosphatases regulated by GADD34 and CReP.

(B) Mitophagy induction upon BTd and Sal treatment and dependence on HRI. K562 cells were treated with indicated concentrations of BTd or Sal for 24 h, and mitophagy was quantified by flow cytometry (mean ± SD, n = 3).

(C) ISR induction by BTd and Sal. K562 cells were treated with 10 μM BTd or 10 μM Sal for 24 h, and the indicated proteins were analyzed by immunoblotting. For LC3B, the band labeled II is the lipidated form that is induced during autophagy.

(D) Suppression of mitophagy by CReP overexpression. Mitophagy was measured in K562 cells expressing GFP-CReP or control (GFP), after treatment with the indicated compounds.

(E) Mitophagy levels in K562 cells upon 24 h treatment with reagents that activate distinct branches of the ISR. Bottom, immunoblotting of the corresponding samples for p-EIF2α and β-ACTIN (loading control).

(F) Effect of HRI pathway on Sal-induced mitophagy. K562 cells expressing non-targeting (NT) sgRNA or sgRNA against indicated genes were treated with vehicle (DMSO) or Sal, and mitophagy levels were quantified by flow cytometry (mean ± SD, n ≥ 4).

See also Figure S3.

concentrations and durations of CHX did not trigger mitophagy (Figures 2E and S2H). Harringtonine (Htn), a translational inhibitor that traps the ribosome near the initiation site,[24,25] also failed to trigger mitophagy (Figure 2E). Similar to DFP, both compounds effectively suppressed translation, as indicated by a puromycylation assay (Figure S2I).

Pharmacological activation of HRI with BTdCPU[1-[(Benzo[d][1,2,3]thiadiazol-6-yl)-3-(3,4-dichlorophenyl)urea); abbreviated "BTd") resulted in a dose-dependent increase in mitophagy that was highly dependent on HRI (Figures 3A and 3B). Treatment of cells with salubrinal (Sal), an inhibitor of the EIF2α phosphatases containing the regulatory subunits CReP (constitutive reverter of eIF2α phosophorylation; also known as protein phosphatase1 regulatory subunit 15B [PPP1R15B]) and GADD34, also caused HRI-dependent activation of mitophagy (Figures 3A and 3B). Both BTd and Sal treatments were associated with accumulation of ATF4 and p-EIF2α protein levels, as well as lipidation of microtubule-associated protein 1 light chain 3 beta (LC3B), a marker for autophagy (Figure 3C). Consistent with the Sal result, overexpression of its target CReP markedly suppressed DFP-induced mitophagy (Figures 3D and S3A). The opposing results with Sal and CReP suggest that the level of p-EIF2α controls the level of mitophagy. Other drugs that have been reported to activate the HRI branch (bortezomib, MG132, and sodium arsenite) also showed mitophagy inducing activity, although BTd was more effective (Figures S3B and S3C).

With evidence that the central outputs of the ISR do not regulate mitophagy, we sought to determine whether mitophagy is specific to the HRI branch. There are four ISR branches, each controlled by a distinct kinase tailored to sense specific stresses.[4,14] Besides HRI, the other kinases are double-stranded RNA-dependent protein kinase (PKR), PKR-like ER kinase (PERK), and GCN2 (Figure 3A). Responding to different stresses, these kinases all phosphorylate EIF2 on serine 51 of the EIF2α subunit to inhibit global protein synthesis. Pharmacological activation of ISR signaling can be achieved by increasing the level of EIF2α phosphorylation, either by activating one of the four EIF2α kinases or by inhibiting EIF2α dephosphorylation with Sal (Figure 3A). We compared the HRI activator BTd to drugs activating the three other EIF2α kinases (1H-Benzimidazole-1-ethanol, 2,3-dihydro-2-imino-alpha-[phenoxymethyl]-3-[phenylmethyl]-monohydrochloride [BEPP]), PKR; CCT020312 [(CCT]), PERK; and histidinol [Hst], GCN2). Thapsigargin (Tg) and tunicamycin (Tun), which are inducers of endoplasmic reticulum (ER) stress, were used as alternative drugs to activate the PERK branch. Whereas BTd, Sal, and DFP treatment substantially increased mitophagy, the other EIF2α kinase activators as well as Tg and Tun did not increase mitophagy over background (Figure 3E). However, all the ISR inducers were effective in elevating p-EIF2α, indicating successful induction of the ISR. These results are consistent with the results from the CRISPRi screen, which identified HRI but none of the other three EIF2α kinases (Figure 2C). Consistent with reports linking these EIF2α kinases with autophagy,[26–29] the inducers all caused increases in LC3B lipidation; however, they failed to induce mitophagy above the control cells even in the presence of EIF2B knockdown (Figures S3D and S3E).

Because HRI is the only branch of the ISR capable of inducing mitophagy, we wondered whether the ability of Sal to induce mitophagy in the absence of DFP was due to basal HRI activity in K562 cells. We found that HRI knockdown abolished the ability of Sal to induce mitophagy (Figure 3F). By contrast, knockdown of DELE1, which mediates elevated levels of HRI activity, did not reduce Sal-induced mitophagy. In addition, knockdown of

Please cite this article in press as: Chakrabarty et al., The HRI branch of the integrated stress response selectively triggers mitophagy, Molecular Cell (2024), https://doi.org/10.1016/j.molcel.2024.01.016

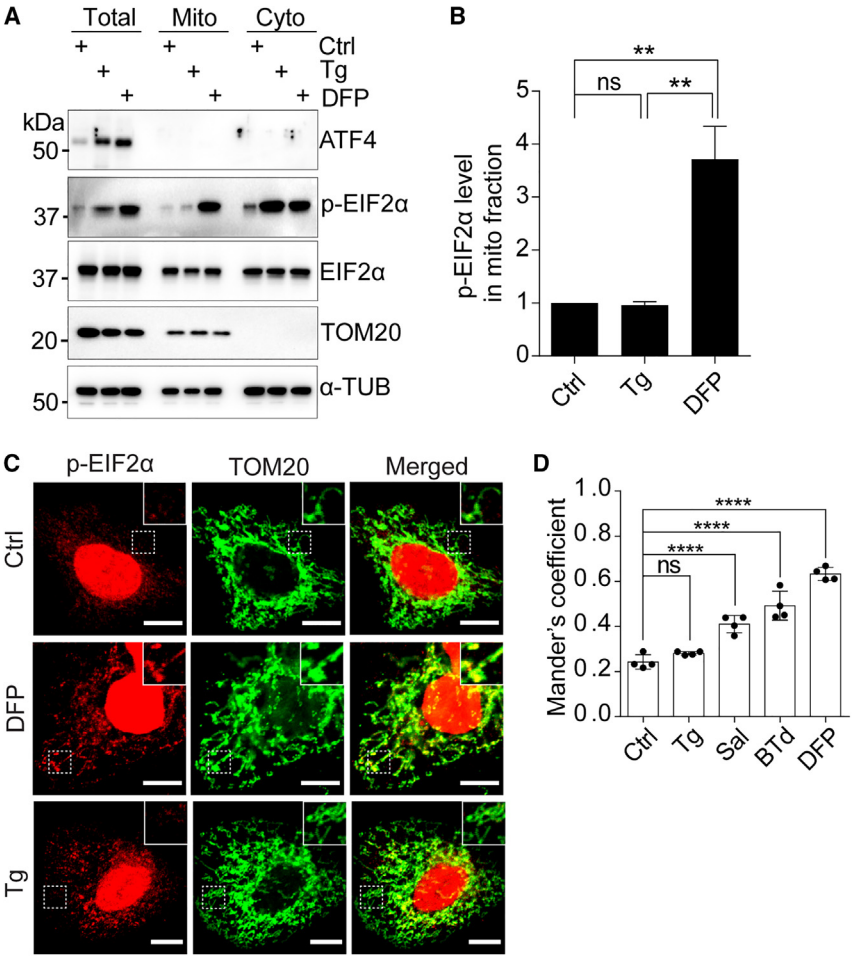

Figure 4. Recruitment of p-EIF2α to mitochondria triggers mitophagy

(A) Biochemical localization of p-EIF2α to mitochondria after DFP treatment. After the indicated treatments, K562 cells were lysed, and mitochondrial (Mito) and cytosolic fractions (Cyto) were analyzed by immunoblotting. TOM20, mitochondrial marker; α-TUB, loading control.

(B) Quantification of p-EIF2α mitochondrial localization. Mitochondrial localization was analyzed as in (A) and quantified by densitometry (mean ± SD, n = 3). Values plotted were normalized to control cells.

(C) Immunofluorescent staining of p-EIF2α during DFP-induced mitophagy. HeLa cells were treated with DMSO, 2 μM Tg, or 1 mM DFP for 24 h and analyzed with antibodies against p-EIF2α and TOM20. Insets shows magnified image of the boxed area.

(D) Quantification of the colocalization between p-EIF2α and TOM20 signals (mean ± SD, n = 10). The mean Mander's coefficient was calculated from 10 images per experiment, and two-way ANOVA was used for statistical analysis from 4 independent experiments.

See also Figure S4.

EIF2B3 or EIF2B4, subunits of the EIF2 GEF, caused dramatic enhancement of mitophagy, with or without Sal. These results indicate that K562 cells have substantial basal activity of HRI that is independent of DELE1. This basal HRI activity allows mitophagy to be induced by inhibition of EIF2α dephosphorylation by Sal.

HRI activation results in mitochondrial localization of p-EIF2

Our results show that only the HRI branch induces mitophagy and that this induction is independent of the central outputs of the ISR. Moving upstream along the ISR pathway, there are two possibilities for specialization of the HRI branch. HRI could phosphorylate another key substrate besides EIF2α, or p-EIF2α generated by HRI could have different properties compared with p-EIF2α generated by the other EIF2α kinases. Our observation that EIF2B is a negative regulator of DFP-mediated mitophagy strongly suggests that regulation occurs at the level of p-EIF2α rather than the kinase. EIF2B strongly binds p-EIF2, and its GEF activity is inhibited by complex formation. Under DFP treatment, EIF2B knockdown would increase the level of free p-EIF2. Moreover, the observations that the phosphatase inhibitor Sal triggers mitophagy and the phosphatase regulator CReP suppresses mitophagy indicate that the phosphorylation state of EIF2α is tightly linked to the level of mitophagy. Interestingly, the ISR inhibitor ISRIB, which does not affect p-EIF2α levels,[30] had no effect on DFP-induced mitophagy (Figure S3F).

Because it has been reported that active DELE1 can be associated with the outer mitochondrial membrane (OMM),[15] we speculated that the HRI pathway may result in accumulation of p-EIF2 on the mitochondrion. To test this hypothesis, we used biochemical fractionation to examine the subcellular localization of p-EIF2α in DFP-treated cells versus control cells and Tg-treated cells. Both DFP and Tg induced the ISR, as indicated by increased p-EIF2α and ATF4 in total cell lysates. However, DFP treatment resulted in notable accumulation of p-EIF2α in the mitochondrial fraction, whereas Tg treatment resulted in p-EIF2α localization almost exclusively in the cytosolic fraction (Figure 4A). Total EIF2α levels were similar across different treatments in the mitochondrial fraction. Quantification indicated a severalfold increase in the mitochondrial p-EIF2α level upon DFP treatment (Figure 4B). We found a similar enrichment of p-EIF2α in the mitochondrial fraction of HeLa cells (Figure S4B). Analysis of the subcellular fractions with an ER marker showed no evidence of ER enrichment of p-EIF2α upon DFP treatment (Figure S4C).

To independently test for mitochondrial localization, we examined the subcellular localization of p-EIF2α by immunofluorescence. We observed clear colocalization of p-EIF2α with the OMM marker TOM20 in DFP-treated samples as opposed to control or Tg-treated samples (Figure 4C). Not all p-EIF2α puncta colocalized with mitochondria, so there may be non-mitochondrial localization of p-EIF2α also. In these experiments, we briefly

Please cite this article in press as: Chakrabarty et al., The HRI branch of the integrated stress response selectively triggers mitophagy, Molecular Cell (2024), https://doi.org/10.1016/j.molcel.2024.01.016

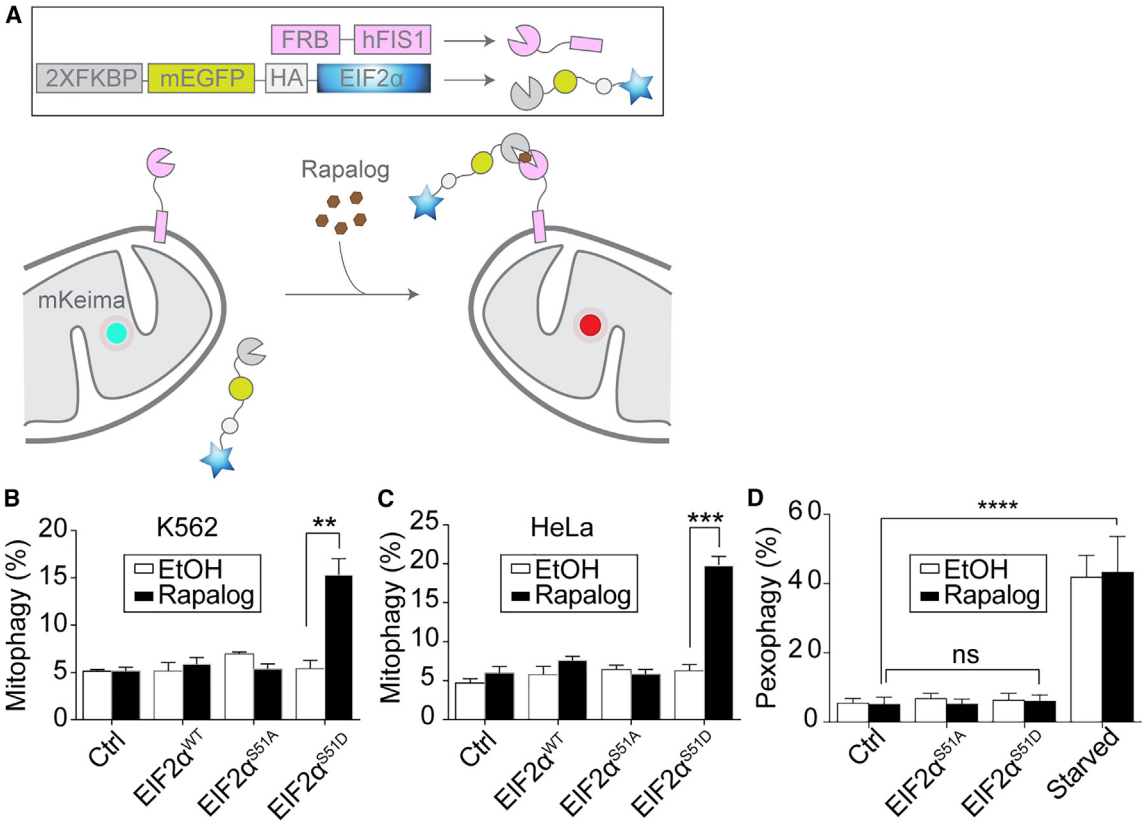

Figure 5. Recruitment of phosphomimetic EIF2α to mitochondria is sufficient to induce mitophagy

(A) Schematic of experimental system for induced tethering of EIF2α to mitochondria. The top rectangle shows the two constructs that are expressed. The FRB-hFis1 fusion protein is expressed on the OMM due to the mitochondrial targeting sequence of hFis1. The EIF2α fusion protein is cytosolic until rapalog is added. Rapalog mediates heterodimerization between FKBP and FRB, thereby bringing the FKBP-GFP-HA-EIF2α fusion protein to the mitochondrial surface.

(B) Mitophagy induction in K562 cells upon recruitment of EIF2α to mitochondria. Control cells or cells expressing EIF2α^{WT}, EIF2α^{S51A} (phosphomutant), or EIF2α^{S51D} (phosphomimetic) were treated with ethanol (EtOH, vehicle) or rapalog and then analyzed for mitophagy by flow cytometry. For (B)–(D), mean ± SD is shown; n = 3.

(C) Mitophagy induction in HeLa cells expressing EIF2 conditionally tethered to mitochondria by FRB-FKBP system. Experiment was performed as in (B), except that HeLa cells were used.

(D) Similar to (B), except cells contained EIF2α targeted to peroxisomes by rapalog, due to expression of FRB fused to the peroxisomal targeting sequence of PEX26. Cells also contained peroxisomally targeted mKeima, a reporter for pexophagy.

See also Figure S5.

permeabilized the cells before fixation. This step disrupts ER structure, so we could not directly test for ER localization in the same experiment. However, mitochondrial structures in non-permeabilized cells could be readily distinguished from the endoplasmic reticulum (Figure S4A). Using the Mander's coefficient to quantify colocalization of p-EIF2α and TOM20 staining, we found a significant increase in colocalization of p-EIF2α with mitochondria in DFP-treated samples (Figure 4D). Analogous results were observed for Sal- and BTd-treated HeLa cells (Figures 4D and S4D). Therefore, the orthogonal approaches of biochemical fractionation and immunostaining support a mitochondrial enrichment of p-EIF2α.

Mitochondrial localization of p-EIF2 is sufficient to trigger mitophagy

These results favor a model where accumulation of p-EIF2 on mitochondria is a signal for mitophagy during HRI activation. To directly test this model, we set up a system in which different forms of EIF2α could be conditionally tethered to the mitochondrial surface. We took advantage of the ability of rapamycin and its analogs (rapalogs) to induce heterodimer formation between the FK506 binding protein (FKBP) and the FKBP-rapamycin binding (FRB) domain of the mammalian target of rapamycin (mTOR).[31,32] We prepared K562 cells expressing FKBP-GFP-HA-EIF2α fusion constructs containing wild-type (WT), phosphomimetic (S51D), or phosphomutant (S51A) EIF2α, along with co-expression of FRB-Fis1 (FRB anchored to the outer mitochondrial membrane [OMM]) (Figure 5A). As expected, clear mitochondrial localization of the FKBP-GFP-HA-EIF2α fusion was induced upon addition of rapalog (Figures S5A and S5B). Accompanying this mitochondrial localization, a substantial increase in mitophagy was measured in K562 cells expressing EIF2α^{S51D} but not in cells expressing EIF2α^{WT} or EIF2α^{S51A} (Figure 5B). Importantly, EIF2α^{S51D}

Please cite this article in press as: Chakrabarty et al., The HRI branch of the integrated stress response selectively triggers mitophagy, Molecular Cell (2024), https://doi.org/10.1016/j.molcel.2024.01.016

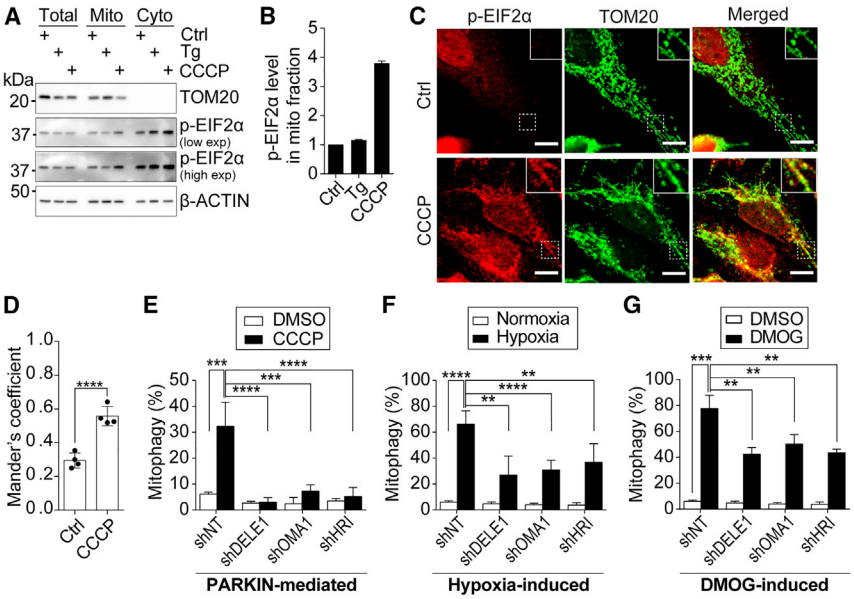

Figure 6. HRI is broadly required for mitophagy

(A) Biochemical localization of p-EIF2α to mitochondria during PARKIN-mediated mitophagy. HeLa cells expressing PARKIN were treated with Tg or CCCP for 4 h, and subcellular fractionation was performed to obtain a mitochondrial and cytosolic fraction. Fractions were analyzed by immunoblotting against the indicated proteins. CCCP induces PARKIN-mediated mitophagy.

(B) Quantification of results in (A) (mean ± SD, n = 2). Values plotted were normalized to control cells.

(C) Immunofluorescent analysis of p-EIF2α during PARKIN-mediated mitophagy.

(D) Quantification of colocalization of p-EIF2α with mitochondria using Mander's coefficient, performed as in Figure 4D.

(E) Effect of HRI components on PARKIN-mediated mitophagy. PARKIN-HeLa cells expressing the indicated shRNA were treated with vehicle (DMSO) or 10 μM CCCP for 24 h. Mitophagy was quantified by flow cytometry (mean ± SD, n ≥ 3).

(F and G) Effect of HRI components on hypoxia-induced (F) and DMOG-induced mitophagy (G). HeLa cells expressing shRNA against the indicated genes were induced to undergo mitophagy. Mitophagy was quantified by flow cytometry (mean ± SD, n ≥ 3).

See also Figure S6.

triggered mitophagy only upon rapalog addition. Similar observations were also observed for HeLa cells expressing these constructs (Figure 5C). Taken together, these results indicate that phosphorylation and mitochondrial localization of EIF2α are necessary and sufficient to trigger mitophagy.

To determine whether p-EIF2α recruitment is sufficient to trigger autophagic degradation of any organelle, we set up an analogous system to target p-EIF2α to peroxisomes. Although rapalog treatment successfully caused peroxisomal targeting (Figure S5C), it failed to induce pexophagy, in contrast to starvation (Figure 5D). These results suggest that some feature of mitochondria, in addition to p-EIF2α targeting, is required for organellar degradation.

HRI activation is important for other forms of mitophagy

Although we discovered the role of HRI in DFP-mediated mitophagy, which is PARKIN-independent,[8] we wondered whether this pathway is relevant for other forms of mitophagy. Due to its relevance to Parkinson's disease, PARKIN-dependent mitophagy is the most widely studied pathway for mitochondrial degradation.[1] To trigger PARKIN-mediated mitophagy, we treated HeLa cells stably expressing PARKIN with CCCP (carbonyl cyanide 3-chlorophenylhydrazone) to disrupt the mitochondrial membrane potential. PARKIN-mediated mitophagy was associated with activation of the HRI branch, as indicated by generation of p-EIF2α and the cleaved form of DELE1 (Figures 6A, S6A, and S6B).[6,7] We found accumulation of p-EIF2α with mitochondria by both biochemical fractionation (Figures 6A, 6B, and S6C) and immunofluorescence (Figures 6C and 6D). Knockdown of DELE1, HRI, or OMA1 suppressed mitophagy to baseline (Figure 6E), indicating that the HRI branch is essential for PARKIN mitophagy.

We also tested the involvement of the HRI branch in hypoxia- and dimethyloxallyl glycine (DMOG, which induces pseudohypoxia)-induced mitophagy, which do not involve PINK1/PARKIN.[33,34] As with PARKIN-mediated mitophagy, hypoxia- and DMOG-induced mitophagy were associated with an increase in p-EIFα that was reduced by HRI and DELE1 knockdown (Figure S6A). It should be noted that a previous study found that DELE1 knockdown prevented HRI activation but did not reduce p-EIF2α levels.[7] This discrepancy could be due to the specific stress conditions used. Hypoxia- and DMOG-induced mitophagy were substantially reduced by knockdown of DELE1, HRI, and OMA1 (Figures 6F and 6G). They were also associated with p-EIF2α accumulating on mitochondria (Figures S6D and S6E).

HRI-mediated mitophagy is mechanistically distinct from ubiquitin-mediated mitophagy

The finding that HRI is important for PARKIN-mediated mitophagy provides an opportunity to determine the stage of mitophagy at which HRI functions, given that this form of mitophagy has been well-characterized. We found that HRI inhibition did not prevent either PARKIN recruitment to mitochondria (Figure 7A) or PINK1 accumulation (Figure 7B). In addition, it did not prevent accumulation of phospho-ubiquitin, a hallmark of PARKIN-mediated mitophagy (Figure 7B). HRI inhibition did not prevent formation of LC3B-GFP puncta with CCCP treatment (Figure S7A). However, it did result in a clear reduction in the association of LC3B-GFP with mitochondria, indicating a defect in the recruitment of autophagosomes to mitochondria (Figures 7C and S7A). A similar defect in recruitment of LC3B-GFP puncta to mitochondria was observed for DFP-induced mitophagy (Figures 7C and S7B). Taken together, these results show that

Please cite this article in press as: Chakrabarty et al., The HRI branch of the integrated stress response selectively triggers mitophagy, Molecular Cell (2024), https://doi.org/10.1016/j.molcel.2024.01.016

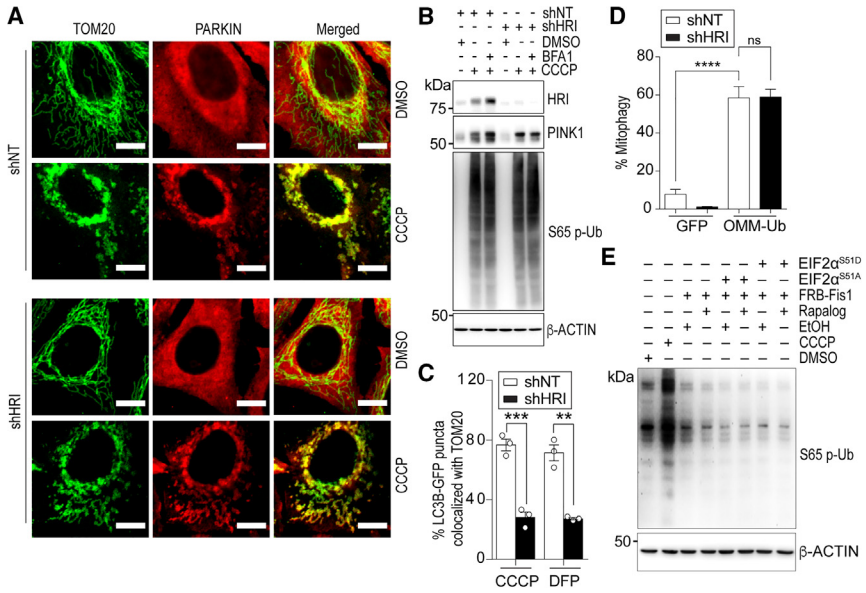

Figure 7. HRI and PINK1/PARKIN pathways are mechanistically distinct

(A) Subcellular localization of PARKIN, after application of CCCP. PARKIN-expressing HeLa cells were transduced with control (NT) shRNA or shRNA against HRI and treated with vehicle or CCCP for 1 h. TOM20 is a mitochondrial marker.

(B) PINK1 and phospho-ubiquitin levels in HeLa cells. Cells expressed control or HRI shRNAs and were treated with vehicle or CCCP as indicated. BFA1 was used to block autophagy.

(C) Colocalization of LC3B-GFP, a marker for autophagosomes, with TOM20 (mitochondria). Cells expressed control or HRI shRNAs and were treated with CCCP or DFP as indicated. The JACoP (Just Another Colocalization Plugin) plugin of Fiji was used to determine colocalization.

(D) Effect of HRI on mitophagy levels of cells expressing ubiquitin chains targeted to the mitochondrial surface. HeLa cells constitutively expressing the indicated shRNAs were transiently transfected with mitochondrial EGFP or OMM-2Ub-KO, a plasmid expressing a dual ubiquitin chain targeted to the OMM.[35] Mitophagy was quantified by flow cytometry (mean ± SD, n ≥ 3).

(E) Phospho-ubiquitin levels in K562 cells upon recruitment of phosphomimetic EIF2α to mitochondria. Cells expressing FRB-Fis1, or FRB-Fis1 with EIF2α^{S51A} or EIF2α^{S51D}, were treated with vehicle (EtOH) or rapalog, and then analyzed by western blotting for phospho-ubiquitin. ACTIN was used as loading control. See also Figure S7.

HRI is not required for the sensing and marking of defective mitochondria. However, recruitment of autophagosomes to the marked mitochondria is reduced in the absence of HRI function.

It is important to determine whether HRI and PINK1/PARKIN function in the same or separate biochemical pathways. We used a previously reported system to overexpress ubiquitin chains on the OMM, which mimics the key output of the PINK1/PARKIN pathway.[35] The ubiquitin chains were sufficient to drive mitophagy, and HRI knockdown was unable to block this effect (Figure 7D). In addition, the induction of mitophagy by recruitment of phosphomimetic eIF2α to mitochondria was not associated with an increase in phospho-ubiquitin (Figure 7E). Therefore, along with PINK1/PARKIN, HRI is required for CCCP induction of mitophagy, and the two pathways are mechanistically distinct.

DISCUSSION

The ISR has four kinases that act as sensors for distinct cellular stresses. These four ISR branches all cause the dual outputs of global reduction in protein translation and activation of ATF4 translation. However, these two common outputs do not affect mitophagy. We found that HRI is the only one out of the four branches that promotes mitophagy, consistent with its ability to sense mitochondrial stress.[6,7] This observation indicates that the output of the ISR can be tailored to the specific stress. Of note, the GCN2 branch of the ISR has been shown to be activated with certain forms of mitochondrial dysfunction,[5] but we did not detect activation of mitophagy by this branch.

Our results suggest that the level of p-EIF2 is critical for mitophagy. This concept is supported by the ability of Sal, an EIF2α phosphatase inhibitor, to activate mitophagy. Conversely, overexpression of the EIF2α phosphatase regulator CReP suppressed mitophagy. We also identified multiple subunits of EIF2B as inhibitors of DFP-induced mitophagy in our CRISPRi screen. Because EIF2B and p-EIF2 form a stable complex, we suggest that EIF2B sequesters p-EIF2 into a complex that is inactive for mitophagy. Although the level of p-EIF2α is critical, simply increasing EIF2 phosphorylation is not sufficient, as evidenced by the inability of non-HRI kinases to induce mitophagy. The HRI branch uniquely triggers mitophagy due to the generation of p-EIF2 on mitochondria. The HRI branch responds to mitochondrial stress by cleaving and releasing DELE1 from mitochondria.[6,7] DFP treatment has been recently reported to additionally stall the import of DELE1 into mitochondria, causing accumulation of full-length DELE1 on the mitochondrial surface.[15] Our subcellular fractionation experiments (Figure S6B) suggest that both long and short forms of DELE1 are largely associated with mitochondria. DELE1 and HRI have been shown to physically interact on the surface of mitochondria,[15] providing an attractive explanation for how activation of the HRI pathway would cause phosphorylation of EIF2α on mitochondria. Further analysis of DELE1, HRI, and EIF2α trafficking will yield further mechanistic understanding of how mitochondrial accumulation of p-EIF2α occurs. The ability of our FRB-FKBP system to conditionally activate mitophagy indicates that the targeting of p-EIF2 to mitochondria is sufficient to drive mitophagy. Therefore, the HRI pathway has co-opted a translation initiation factor into a second role as a mitophagy signal. However, the targeting of p-EIF2 to peroxisomes did not induce pexophagy, indicating that some additional feature of mitochondria, along with p-EIF2 localization, is involved in promoting organellar degradation.

Although we initiated these studies using a PARKIN-independent form of mitophagy, the HRI pathway plays a critical role in a

broad range of mitophagy conditions. In addition to iron chelation, the HRI pathway is responsible for a substantial portion of the mitophagy induced by PINK1/PARKIN, DMOG, and hypoxia. The involvement of HRI in PINK1/PARKIN-mediated mitophagy is notable because this pathway appears to be specialized and distinct from basal mitophagy.[36,37] Although HRI is required for PINK1/PARKIN-mediated mitophagy, many of the early steps involved in marking mitochondria for degradation—including PINK1 accumulation, PARKIN recruitment to mitochondria, and accumulation of phospho-ubiquitin—occur independently of HRI.

It is important to address how HRI inhibition can reduce PINK1/PARKIN mitophagy without affecting accumulation of phospho-ubiquitin, given that ubiquitination of the mitochondrial surface recruits autophagy receptors and has been shown to be sufficient to induce mitophagy.[35,38] Overexpression of ubiquitin chains on the mitochondrial surface mimics the downstream event of PINK1/PARKIN activation that drives mitophagy. We find that HRI inhibition does not interfere with this purely ubiquitin-driven mitophagy. In a related experiment, we show that recruitment of phosphomimetic eIF2α to mitochondria is sufficient to induce mitophagy but does not result in phospho-ubiquitin accumulation. These two experiments mechanistically disentangle PINK1/PARKIN from HRI and suggest they promote separate, parallel pathways of mitophagy.

In most experimental models of PINK1/PARKIN mitophagy, PARKIN is overexpressed, and mitochondrial membrane depolarization is used as the trigger. Under these experimental conditions, we find that the HRI pathway is simultaneously activated and contributes substantially to the final level of mitophagy. When HRI is inhibited, the PINK1/PARKIN system is still able to promote mitochondrial phospho-ubiquitin, but the levels are apparently insufficient to result in much mitophagy. In the previous studies demonstrating that mitophagy could be induced solely by expression of outer membrane ubiquitin chains,[35] the experimental systems were optimized by overexpression and likely generate levels of phospho-ubiquitin or mitophagy receptor recruitment exceeding those under endogenous conditions. Our results show that the DELE1/HRI pathway is activated under a broad range of mitochondrial stresses, including DFP, mitochondrial membrane depolarization, hypoxia, and DMOG. In the case of PINK/PARKIN mitophagy triggered by mitochondrial membrane depolarization, we propose that activation of DELE1/HRI induces a pathway of mitophagy in parallel to that of PINK1/PARKIN. In this view, what is commonly thought to be PINK1/PARKIN-mediated mitophagy actually consists of a component intrinsic to PINK1/PARKIN and a second component mediated by HRI. It remains to be determined whether these pathways act additively or synergistically.

Limitations of the study

Our findings on mitophagy have relied on cultured cells, primarily K562 and HeLa cells. It will be important to examine the role of p-EIF2α in mitophagy in other cell types and in intact tissues with animal models. The use of animal models would also allow the examination of endogenous mitophagy, whereas our studies have utilized artificial triggers, such as DFP, to induce mitophagy. The HRI activator BTd used in this study has recently been shown to additionally cause mitochondrial depolarization.[39] More experiments will be needed to understand the mechanism whereby p-EIF2 on the mitochondrial surface results in recruitment or initiation of autophagosomes. In particular, it will likely be important to identify binding partners of p-EIF2 on mitochondria. Finally, it remains possible that mitochondrial p-EIF2 has effects on the translation of mitochondrially localized proteins whose mRNAs are translated close to the mitochondrial surface.[40–42]

STAR★METHODS

Detailed methods are provided in the online version of this paper and include the following:

- KEY RESOURCES TABLE
- RESOURCE AVAILABILITY
  - Lead contact
  - Materials availability
  - Data and code availability
- EXPERIMENTAL MODEL AND STUDY PARTICIPANT DETAILS
  - Cell culture and generation of cell lines
- METHOD DETAILS
  - Plasmids
  - Drug, hypoxia, and starvation treatments
  - Lentiviral and retroviral transduction
  - Antibodies
  - Puromycylation assay
  - Flow cytometry
  - qPCR
  - Confocal microscopy and post-imaging processing
  - Sample preparation for immunofluorescence
  - Rapalog-induced FRB-FKBP dimerization assay
  - CRISPRi screen
  - Subcellular fractionation
- QUANTIFICATION AND STATISTICAL ANALYSIS
- ADDITIONAL RESOURCES

SUPPLEMENTAL INFORMATION

Supplemental information can be found online at https://doi.org/10.1016/j.molcel.2024.01.016.

ACKNOWLEDGMENTS

We are grateful to A. Merchan, J. Repogle, J. Weissman, K. Page, R. She, and R. Voorhees for encouragement and advice on CRISPRi screening; D. Perez, J. Tijerina, and R. Diamond (Caltech Flow Cytometry and Cell Sorting Facility) for support with flow cytometry and FACS experiments; and I. Antoshechkin (Millard and Muriel Jacobs Genetics and Genomics Laboratory, Caltech) for support with next-generation sequencing. We thank the following investigators for contribution of important reagents: L. Jae, S. Yamashita, K. Yamano, N. Matsuda, G. Varuzhanyan, R. Youle, A. Ting, M. Moore, D. Ron, and J. Lippincott-Schwartz. We thank members of the Chan lab for helpful discussions and comments on the manuscript. This work was funded by the National Institutes of Health grant R35 GM127147 (D.C.C.).

AUTHOR CONTRIBUTIONS

Conceptualization, Y.C. and D.C.C.; methodology, Y.C., Z.Y., and H.C.; investigation, Y.C., Z.Y., and H.C.; funding acquisition, D.C.C.; supervision, D.C.C.; writing – original draft, Y.C. and D.C.C.; writing – review & editing, Y.C., D.C.C., Z.Y., and H.C.

DECLARATION OF INTERESTS

The authors declare no competing interests.

Received: December 16, 2022
Revised: August 31, 2023
Accepted: January 18, 2024
Published: February 9, 2024

REFERENCES

1. Pickles, S., Vigié, P., and Youle, R.J. (2018). Mitophagy and Quality Control Mechanisms in Mitochondrial Maintenance. Curr. Biol. *28*, R170–R185.
2. Onishi, M., Yamano, K., Sato, M., Matsuda, N., and Okamoto, K. (2021). Molecular mechanisms and physiological functions of mitophagy. EMBO J. *40*, e104705.
3. Narendra, D., Tanaka, A., Suen, D.-F., and Youle, R.J. (2008). Parkin is recruited selectively to impaired mitochondria and promotes their autophagy. J. Cell Biol. *183*, 795–803.
4. Costa-Mattioli, M., and Walter, P. (2020). The integrated stress response: From mechanism to disease. Science *368*, eaat5314.
5. Mick, E., Titov, D.V., Skinner, O.S., Sharma, R., Jourdain, A.A., and Mootha, V.K. (2020). Distinct mitochondrial defects trigger the integrated stress response depending on the metabolic state of the cell. eLife *9*, e49178.
6. Fessler, E., Eckl, E.-M., Schmitt, S., Mancilla, I.A., Meyer-Bender, M.F., Hanf, M., Philippou-Massier, J., Krebs, S., Zischka, H., and Jae, L.T. (2020). A pathway coordinated by DELE1 relays mitochondrial stress to the cytosol. Nature *579*, 433–437.
7. Guo, X., Aviles, G., Liu, Y., Tian, R., Unger, B.A., Lin, Y.-H.T., Wiita, A.P., Xu, K., Correia, M.A., and Kampmann, M. (2020). Mitochondrial stress is relayed to the cytosol by an OMA1-DELE1-HRI pathway. Nature *579*, 427–432.
8. Allen, G.F.G., Toth, R., James, J., and Ganley, I.G. (2013). Loss of iron triggers PINK1/Parkin-independent mitophagy. EMBO Rep. *14*, 1127–1135.
9. Horlbeck, M.A., Gilbert, L.A., Villalta, J.E., Adamson, B., Pak, R.A., Chen, Y., Fields, A.P., Park, C.Y., Corn, J.E., Kampmann, M., et al. (2016). Compact and highly active next-generation libraries for CRISPR-mediated gene repression and activation. eLife *5*, e19760.
10. Gilbert, L.A., Horlbeck, M.A., Adamson, B., Villalta, J.E., Chen, Y., Whitehead, E.H., Guimaraes, C., Panning, B., Ploegh, H.L., Bassik, M.C., et al. (2014). Genome-Scale CRISPR-Mediated Control of Gene Repression and Activation. Cell *159*, 647–661.
11. Gilbert, L.A., Larson, M.H., Morsut, L., Liu, Z., Brar, G.A., Torres, S.E., Stern-Ginossar, N., Brandman, O., Whitehead, E.H., Doudna, J.A., et al. (2013). CRISPR-mediated modular RNA-guided regulation of transcription in eukaryotes. Cell *154*, 442–451.
12. Wang, C. (2020). A Sensitive and Quantitative mKeima Assay for Mitophagy via FACS. Curr. Protoc. Cell Biol. *86*, e99.
13. Sun, N., Malide, D., Liu, J., Rovira, I.I., Combs, C.A., and Finkel, T. (2017). A fluorescence-based imaging method to measure in vitro and in vivo mitophagy using mt-Keima. Nat. Protoc. *12*, 1576–1587.
14. Girardin, S.E., Cuziol, C., Philpott, D.J., and Arnoult, D. (2021). The eIF2α kinase HRI in innate immunity, proteostasis, and mitochondrial stress. FEBS Journal *288*, 3094–3107.
15. Sekine, Y., Houston, R., Eckl, E.-M., Fessler, E., Narendra, D.P., Jae, L.T., and Sekine, S. (2023). A mitochondrial iron-responsive pathway regulated by DELE1. Mol. Cell *83*, 2059–2076.e6.
16. Gordiyenko, Y., Llácer, J.L., and Ramakrishnan, V. (2019). Structural basis for the inhibition of translation through eIF2α phosphorylation. Nat. Commun. *10*, 2640. https://www.nature.com/articles/s41467-019-10606-1.
17. Kashiwagi, K., Yokoyama, T., Nishimoto, M., Takahashi, M., Sakamoto, A., Yonemochi, M., Shirouzu, M., and Ito, T. (2019). Structural basis for eIF2B inhibition in integrated stress response. Science *364*, 495–499.
18. Kenner, L.R., Anand, A.A., Nguyen, H.C., Myasnikov, A.G., Klose, C.J., McGeever, L.A., Tsai, J.C., Miller-Vedam, L.E., Walter, P., and Frost, A. (2019). eIF2B-catalyzed nucleotide exchange and phosphoregulation by the integrated stress response. Science *364*, 491–495.
19. Zhao, J.-F., Rodger, C.E., Allen, G.F.G., Weidlich, S., and Ganley, I.G. (2020). HIF1α-dependent mitophagy facilitates cardiomyoblast differentiation. Cell Stress *4*, 99–113.
20. Kravic, B., Harbauer, A.B., Romanello, V., Simeone, L., Vögtle, F.-N., Kaiser, T., Straubinger, M., Huraskin, D., Böttcher, M., Cerqua, C., et al. (2018). In mammalian skeletal muscle, phosphorylation of TOMM22 by protein kinase CSNK2/CK2 controls mitophagy. Autophagy *14*, 311–335.
21. Heo, J.-M., Ordureau, A., Swarup, S., Paulo, J.A., Shen, K., Sabatini, D.M., and Harper, J.W. (2018). RAB7A phosphorylation by TBK1 promotes mitophagy via the PINK-PARKIN pathway. Sci. Adv. *4*, eaav0443.
22. Lazarou, M., Sliter, D.A., Kane, L.A., Sarraf, S.A., Wang, C., Burman, J.L., Sideris, D.P., Fogel, A.I., and Youle, R.J. (2015). The ubiquitin kinase PINK1 recruits autophagy receptors to induce mitophagy. Nature *524*, 309–314.
23. Rainbolt, T.K., Atanassova, N., Genereux, J.C., and Wiseman, R.L. (2013). Stress-regulated translational attenuation adapts mitochondrial protein import through Tim17A degradation. Cell Metab. *18*, 908–919.
24. Ingolia, N.T., Lareau, L.F., and Weissman, J.S. (2011). Ribosome Profiling of Mouse Embryonic Stem Cells Reveals the Complexity and Dynamics of Mammalian Proteomes. Cell *147*, 789–802.
25. Huang, M.-T. (1975). Harringtonine, an Inhibitor of Initiation of Protein Biosynthesis. Mol. Pharmacol. *11*, 511–519.
26. Tallóczy, Z., Jiang, W., Virgin, H.W., Leib, D.A., Scheuner, D., Kaufman, R.J., Eskelinen, E.-L., and Levine, B. (2002). Regulation of starvation- and virus-induced autophagy by the eIF2α kinase signaling pathway. Proc. Natl. Acad. Sci. USA *99*, 190–195.
27. Tallóczy, Z., Virgin, H.W., and Levine, B. (2006). PKR-dependent autophagic degradation of herpes simplex virus type 1. Autophagy *2*, 24–29.
28. Ren, H., Zhai, W., Lu, X., and Wang, G. (2021). The Cross-Links of Endoplasmic Reticulum Stress, Autophagy, and Neurodegeneration in Parkinson's Disease. Front. Aging Neurosci. *13*, 691881.
29. Maurin, A.-C., Parry, L., B'chir, W., Carraro, V., Coudy-Gandilhon, C., Chaouki, G., Chaveroux, C., Mordier, S., Martinie, B., Reinhardt, V., et al. (2022). GCN2 upregulates autophagy in response to short-term deprivation of a single essential amino acid. Autophagy Rep. *1*, 119–142.
30. Sekine, Y., Zyryanova, A., Crespillo-Casado, A., Fischer, P.M., Harding, H.P., and Ron, D. (2015). Stress responses. Mutations in a translation initiation factor identify the target of a memory-enhancing compound. Science *348*, 1027–1030.
31. Rivera, V.M., Clackson, T., Natesan, S., Pollock, R., Amara, J.F., Keenan, T., Magari, S.R., Phillips, T., Courage, N.L., Cerasoli, F., et al. (1996). A humanized system for pharmacologic control of gene expression. Nat. Med. *2*, 1028–1032.
32. Liberles, S.D., Diver, S.T., Austin, D.J., and Schreiber, S.L. (1997). Inducible gene expression and protein translocation using nontoxic ligands identified by a mammalian three-hybrid screen. Proc. Natl. Acad. Sci. USA *94*, 7825–7830.
33. Liu, L., Feng, D., Chen, G., Chen, M., Zheng, Q., Song, P., Ma, Q., Zhu, C., Wang, R., Qi, W., et al. (2012). Mitochondrial outer-membrane protein

FUNDC1 mediates hypoxia-induced mitophagy in mammalian cells. Nat. Cell Biol. *14*, 177–185.

34. Hu, S., Zhang, C., Ni, L., Huang, C., Chen, D., Shi, K., Jin, H., Zhang, K., Li, Y., Xie, L., et al. (2020). Stabilization of HIF-1α alleviates osteoarthritis via enhancing mitophagy. Cell Death Dis. *11*, 481.
35. Yamano, K., Kikuchi, R., Kojima, W., Hayashida, R., Koyano, F., Kawawaki, J., Shoda, T., Demizu, Y., Naito, M., Tanaka, K., et al. (2020). Critical role of mitochondrial ubiquitination and the OPTN-ATG9A axis in mitophagy. J. Cell Biol. *219*, e201912144.
36. Lee, J.J., Sanchez-Martinez, A., Martinez Zarate, A., Benincá, C., Mayor, U., Clague, M.J., and Whitworth, A.J. (2018). Basal mitophagy is widespread in Drosophila but minimally affected by loss of Pink1 or parkin. J. Cell Biol. *217*, 1613–1622.
37. McWilliams, T.G., Prescott, A.R., Montava-Garriga, L., Ball, G., Singh, F., Barini, E., Muqit, M.M.K., Brooks, S.P., and Ganley, I.G. (2018). Basal Mitophagy Occurs Independently of PINK1 in Mouse Tissues of High Metabolic Demand. Cell Metab. *27*, 439–449.e5.
38. Goodall, E.A., Kraus, F., and Harper, J.W. (2022). Mechanisms underlying ubiquitin-driven selective mitochondrial and bacterial autophagy. Mol. Cell *82*, 1501–1513.
39. Perea, V., Baron, K.R., Dolina, V., Aviles, G., Kim, G., Rosarda, J.D., Guo, X., Kampmann, M., and Wiseman, R.L. (2023). Pharmacologic activation of a compensatory integrated stress response kinase promotes mitochondrial remodeling in PERK-deficient cells. Cell Chem. Biol. *30*, 1571–1584.e5.
40. Williams, C.C., Jan, C.H., and Weissman, J.S. (2014). Targeting and plasticity of mitochondrial proteins revealed by proximity-specific ribosome profiling. Science *346*, 748–751.
41. Gao, J., Schatton, D., Martinelli, P., Hansen, H., Pla-Martin, D., Barth, E., Becker, C., Altmueller, J., Frommolt, P., Sardiello, M., et al. (2014). CLUH regulates mitochondrial biogenesis by binding mRNAs of nuclear-encoded mitochondrial proteins. J. Cell Biol. *207*, 213–223.
42. Schatton, D., and Rugarli, E.I. (2018). A concert of RNA-binding proteins coordinates mitochondrial function. Crit. Rev. Biochem. Mol. Biol. *53*, 652–666.
43. Chan, N.C., Salazar, A.M., Pham, A.H., Sweredoski, M.J., Kolawa, N.J., Graham, R.L.J., Hess, S., and Chan, D.C. (2011). Broad activation of the ubiquitin-proteasome system by Parkin is critical for mitophagy. Hum. Mol. Genet. *20*, 1726–1737.
44. Chen, H., Detmer, S.A., Ewald, A.J., Griffin, E.E., Fraser, S.E., and Chan, D.C. (2003). Mitofusins Mfn1 and Mfn2 coordinately regulate mitochondrial fusion and are essential for embryonic development. J. Cell Biol. *160*, 189–200.
45. Schindelin, J., Arganda-Carreras, I., Frise, E., Kaynig, V., Longair, M., Pietzsch, T., Preibisch, S., Rueden, C., Saalfeld, S., Schmid, B., et al. (2012). Fiji: an open-source platform for biological-image analysis. Nat. Methods *9*, 676–682.
46. Vargas, J.N.S., Wang, C., Bunker, E., Hao, L., Maric, D., Schiavo, G., Randow, F., and Youle, R.J. (2019). Spatiotemporal Control of ULK1 Activation by NDP52 and TBK1 during Selective Autophagy. Mol. Cell *74*, 347–362.e6.
47. Chen, R., Rato, C., Yan, Y., Crespillo-Casado, A., Clarke, H.J., Harding, H.P., Marciniak, S.J., Read, R.J., and Ron, D. (2015). G-actin provides substrate-specificity to eukaryotic initiation factor 2α holophosphatases. eLife *4*, e04871.
48. Bolte, S., and Cordelières, F.P. (2006). A guided tour into subcellular colocalization analysis in light microscopy. J. Microsc. *224*, 213–232.
49. Losón, O.C., Song, Z., Chen, H., and Chan, D.C. (2013). Fis1, Mff, MiD49, and MiD51 mediate Drp1 recruitment in mitochondrial fission. Mol. Biol. Cell *24*, 659–667.
50. Mishra, P., Carelli, V., Manfredi, G., and Chan, D.C. (2014). Proteolytic cleavage of Opa1 stimulates mitochondrial inner membrane fusion and couples fusion to oxidative phosphorylation. Cell Metab. *19*, 630–641.

Please cite this article in press as: Chakrabarty et al., The HRI branch of the integrated stress response selectively triggers mitophagy, Molecular Cell (2024), https://doi.org/10.1016/j.molcel.2024.01.016

STAR★METHODS

KEY RESOURCES TABLE

REAGENT or RESOURCE	SOURCE	IDENTIFIER
Antibodies		
ATF4	Cell Signaling	11815; RRID:AB_2616025
EIF2B3	Novus Biologicals	NBP1-83985; RRID: AB_11016865
EIF2B4	Proteintech	11332-1-AP; RRID: AB_2277640
EIF2α	Cell Signaling	5324; RRID:AB_10692650
Phospho-EIF2α (Ser51)	Cell Signaling	3398; RRID:AB_2096481
GFP	Takara Bio	632380; RRID:AB_10013427
LC3B	Cell Signaling	2775; RRID:AB_915950
OMA1	Santa Cruz	sc-515788; RRID:AB_2905488
HRI	Proteintech	20499-1-AP; RRID:AB_10697665
TIMM50	Proteintech	22229-1-AP; RRID:AB_2879039
TOM20	Santa Cruz	sc-17764; RRID:AB_628381
PINK1	Proteintech	23274-1-AP; RRID:AB_2879244
Phospho-Ubiquitin (Ser65)	Cell Signaling	62802; RRID:AB_2799632
α-Puromycin	Kerafast	EQ0001; RRID:AB_2620162
α-Tubulin	Sigma	T6199; RRID:AB_477583
β-Actin	Sigma	A5441; RRID:AB_476744
HSP60	Santa Cruz	sc-1052; RRID:AB_631683
PEX14	Proteintech	10594-1-AP; RRID:AB_2252194
PARKIN	Proteintech	14060-1-AP; RRID:AB_2878005
LC3B	Cosmo Bio USA	CAC-CTB-LC3-2-IC; RRID:AB_10707197
VDAC1	Abcam	ab15895; RRID:AB_2214787
CALNEXIN	Proteintech	66903-1-Ig; RRID:AB_2882231
anti-mouse IgG AlexaFluor 488	Thermo Fisher	A-21202; RRID:AB_141607
anti-rabbit IgG AlexaFluor 555	Thermo Fisher	A-31572; RRID:AB_162543
anti-goat IgG AlexaFluor 568	Thermo Fisher	A-11057; RRID:AB_2534104
SPRIselect beads	Beckman Coulter	B23318
Chemicals, peptides, and recombinant proteins		
A/C Heterodimerizer, AP21967 ligand (Rapalog)	Takara	635056
Bafilomycin A1	Cayman Chemical	11038
BEPP	Sigma	B2938
BTdCPU	Sigma	324892
Bortezomib	Sigma	5.04314
CCCP	Sigma	C2759
CCT020312	Sigma	324879
Cycloheximide	Sigma	C1988
DFP	Fujifilm Wako Chemicals	324-65151
DMOG	Cayman Chemical	71210
Haemin chloride	Sigma	3741
Harringtonin	Cayman Chemical	15361
Histidinol	Cayman Chemical	18739
ISRIB	Sigma	SML0843
MG132	Sigma	474790
Polybrene	Sigma	H9268

(*Continued on next page*)

Please cite this article in press as: Chakrabarty et al., The HRI branch of the integrated stress response selectively triggers mitophagy, Molecular Cell (2024), https://doi.org/10.1016/j.molcel.2024.01.016

Continued

REAGENT or RESOURCE	SOURCE	IDENTIFIER
Puromycin dihydrochloride	Sigma	P8833
Salubrinal	Sigma	SML0941
Sodium Arsenite	Sigma	S7400
SYTOX Green	Thermo Fisher	S34860
Thapsigargin	Sigma	T9033
Tunicamycin	Sigma	T7765
Z-VAD-FMK	Cayman Chemical	14463
Critical commercial assays		
Lipofectamine 3000 Transfection Reagent kit	Thermo Fisher	L3000008
Nucleospin Blood XL kit	Takara	740950
Experimental models: Cell lines		
K562-dCAS9	Gilbert et al.[11]	N/A
HEK293T	ATCC	CRL-11268; RRID:CVCL_1926
HeLa WT	Chan et al.[43]	N/A
HeLa-hPARKIN	Chan et al.[43]	N/A
Oligonucleotides		
hCRISPRi-v2 pooled half library	Addgene	83969; RRID:Addgene_83969
sgRNA sequences	STAR Methods	N/A
shRNA sequences	STAR Methods	N/A
qPCR primer sequences	STAR Methods	N/A
Recombinant DNA		
eIF2a 1	Addgene	21807; RRID:Addgene_21807
pHAGE-FKBP-GFP-NDP52	Addgene	135296; RRID:Addgene_135296
FLAG_hPPP1R15B_4-713_mCherry_UK1298	Addgene	80707; RRID:Addgene_80707
pLX208 CMV sTurboID (C)-HA-FRB-ERM	Addgene	153007; RRID:Addgene_153007
pUltra	Addgene	24129; RRID:Addgene_24129
CRISPRi/a-v2 vector	Addgene	84832; RRID:Addgene_84832
Sec61b-Emerald	Addgene	90992; RRID:Addgene_90992
pHAGE-FKBP-GFP-HA-EIF2α^{WT}	This study	N/A
pHAGE-FKBP-GFP-HA-EIF2α^{S51D}	This study	N/A
pHAGE-FKBP-GFP-HA-EIF2α^{S51A}	This study	N/A
pLX208 CMV sTurboID (C)-HA-FRB-PEX26	This study	N/A
pQCXIP-mKeima-PTS1	This study	N/A
pMXs-Mito-mKeima	Gifted from Dr. Shunichi Yamashita (Niigata University)	N/A
pHAGE-BFP-P2A-FRB-Fis1	Gifted from Dr. Richard Youle (NINDS)	N/A
pcDNA3.1(+)_T20(1-49)-YFP-2Ub(KO)-3HA	Gifted from Dr. Noriyuki Matsuda (Tokyo Metropolitan Institute of Medical Science)	N/A
DELE1-HA	Gifted from Dr. Lucas Jae (LMU Munich)	N/A
pUltra-CReP-GFP	This study	N/A
pQCXIP-Su9-EGFP	Chen et al.[44]	N/A
pQCXIP-Mito-Dsred2	Chen et al.[44]	N/A
Software and algorithms		
FlowJo Software	Version 10.8	N/A
Image J (Fiji)	Schindelin et al.[45]	N/A
Graphpad Prism	Version 6.07	N/A
CRISPRi screen processing code pipeline	Horlbeck et al.[9] and Gilbert et al.[10]	https://github.com/mhorlbeck/ScreenProcessing

(*Continued on next page*)

Please cite this article in press as: Chakrabarty et al., The HRI branch of the integrated stress response selectively triggers mitophagy, Molecular Cell (2024), https://doi.org/10.1016/j.molcel.2024.01.016

Continued

REAGENT or RESOURCE	SOURCE	IDENTIFIER
Deposited data		
Raw data	This paper	Mendeley Data: https://doi.org/10.17632/vp4w6ghd5w.1
Data from CRISPRi screen	This paper; Table S1	N/A

RESOURCE AVAILABILITY

Lead contact

Further information and requests for resources and reagents should be directed to and will be fulfilled by lead contact, David C. Chan (dchan@caltech.edu).

Materials availability

Plasmids generated in this study will be deposited to Addgene or available from the lead contact.

Data and code availability

- The raw data files for images have been deposited at Mendeley and are publicly available as of the date of publication. The DOI is listed in the key resources table. The dataset from the CRISPRi screen is provided in Table S1.
- This paper does not report original code.
- Any additional information required to reanalyze the data reported in this paper is available from the lead contact upon request.

All data are available in the main text or the supplemental information.

EXPERIMENTAL MODEL AND STUDY PARTICIPANT DETAILS

Cell culture and generation of cell lines

K562 cells were grown in RPMI-1640 with 25 mM HEPES, 2.0 g/L $NaHCO_3$, and 0.3 g/L L-glutamine supplemented with 10% FBS, 2 mM glutamine, 100 units/ml penicillin, and 100 μg/ml streptomycin. Cells were maintained between 0.25-1 x10^6 cells/ml. HEK293T and HeLa cells were grown in DMEM supplemented with 10% FBS, 100 units/ml penicillin and 100 μg/ml streptomycin. All cell lines were grown at 37°C and 5% CO_2.

METHOD DETAILS

Plasmids

For construction of pHAGE-FKBP-GFP-HA-EIF2α, the *EIF2S1* sequence was obtained from the plasmid eIF2a1 (Addgene, 21807). Point mutations were introduced into *EIF2α* with overlap extension PCR-based mutagenesis. PCR primers were designed to add an HA tag at the N terminus of *EIF2S1* sequence. The final inserts were cloned into the SalI/BamHI sites of pHAGE-FKBP-GFP-NDP52 (Addgene, 135296).[46] Plasmids were obtained from the following sources: Mito-mKeima (S. Yamashita); DELE1-HA (L. Jae); pHAGE-BFP-P2A-FRB-Fis1 (R. Youle); pcDNA3.1(+)_T20(1-49)-YFP-2Ub(KO)-3HA (K. Yamano and N. Matsuda)[35]; FLAG_hPPP1R15B_4-713_mCherry_UK1298 (D. Ron).[47]

For creating the peroxisome targeting FRB fragment, pLX208 CMV sTurboID (C)-HA-FRB-ERM (Addgene, 153007) was double digested with MluI and BstBI to remove the ER transmembrane domain and create the linearized backbone. The tail-anchored sequence from PEX26 cDNA was ligated into the backbone.

The CReP-GFP plasmid was made by first linearizing pUltra (Addgene, 24129) by single digestion with AgeI. The CReP sequence was amplified from FLAG_hPPP1R15B_4-713_mCherry_UK1298 (Addgene, 80707) and inserted into the pUltra backbone by Gibson Assembly.

The sgRNAs were generated by cloning of annealed oligonucleotides into the lentiviral CRISPRi/a-v2 vector (Addgene, 84832) digested with BstXI/BlpI.[9] The protospacer sequences were: *DELE1* #1, 5' GAAGCGCGAGACCAACCCTT 3'; *DELE1* #2, 5' GTAGCCGCTGTCCCAAGGGT 3'; *HRI* #1, 5' GATCGGAGTGTGGCAGTGCT 3'; *HRI* #2, 5' GTAGCTGCAGCATCGGAGTG 3'; *EIF2B3*, 5' GAGATCGCTGGGAGCGGTTG 3'; *EIF2B4*, 5' GCTGAGGGCGATGGCTGCTG 3'; *OMA1*, 5' GCGAGTAGGATC GTGCCCAG 3'; *ATF4*, 5' GGACGAAGTCTATAAAGGGC 3'; Non-targeting (NT), 5' GGCTCGGTCCCGCGTCGTCG 5'.

For RNA interference, retroviral transduction was used to express shRNAs from the H1 promoter. The target sequences were: *DELE1*, 5' GCAGAGAGCTGTGAAATATCT 3'; *OMA1*, 5' GGAAGCTATTCCTTGGTTTGA 3'; *HRI*, 5' GCATGAACCAAAC CCACTTCG 3'; *ATF4* #1, 5' GGAGATCCAGTACCTGAAAGA 3'; *ATF4* #2, 5' GATCCAGTACCTGAAAGATTT 3'; Non-targeting (NT), 5' GACTAGAAGGCACAGAGGG 3'.

Please cite this article in press as: Chakrabarty et al., The HRI branch of the integrated stress response selectively triggers mitophagy, Molecular Cell (2024), https://doi.org/10.1016/j.molcel.2024.01.016

Drug, hypoxia, and starvation treatments

Cells were treated with following reagents for 24 h unless otherwise stated: 1000 μM DFP or as specified (Fujifilm Wako Chemicals, 324-65151), 10 μM CCCP (Sigma, C2759), 1000 μM DMOG (Cayman Chemical, 71210), 1 μM bafilomycin A1 (Cayman Chemical, 11038), 1 μM CCT020312 (Sigma, 324879), 2 μM thapsigargin (Sigma, T9033), 10 μM tunicamycin (Sigma, T7765), 500 μM histidinol (Cayman Chemical, 18739), 10 μM BEPP (Sigma, B2938), 10 μM or as specified BTdCPU (Sigma, 324892), 100-1000 nM ISRIB (Sigma, SML0843), 1-50 μg/ml cycloheximide as specified (Sigma, C1988), 10 μM Salubrinal or as specified (Sigma, SML0941), 20 μM Z-VAD-FMK (Cayman Chemical, 14463), 10 μM Harringtonine (Cayman Chemical, 15361), 5 μM Bortezomib (Sigma, 5043140001), 25 μM MG132 (Sigma, 474790), 400 μM sodium arsenite (Sigma, S7400). All CCCP treatments (10 μM) were done in presence of 20 μM Z-VAD-FMK.

For hypoxia experiments, HeLa cells were seeded for 12 h. Cells were fed with fresh media and placed in a hypoxia chamber. 1% O2 was passed through the hypoxia chamber for 5 mins to saturate the hypoxia chamber before quickly closing. For starvation experiments, HeLa cells were grown for 24 h to reach ~70% confluence. Then cells were cultured in fresh media for 12 h before they were washed twice with 1X Hanks' balanced salt solution (HBSS) and finally incubated in 1X HBSS for 4 h.

Lentiviral and retroviral transduction

For stable expression of lentiviral and retroviral constructs in HeLa and K562 cells, the calcium phosphate method was used to transfect HEK293T cells with packaging plasmids (pVSV-G and pΔ8.9; lentiviral) or pUMVC (retroviral), and lentiviral or retroviral expression constructs. Fresh media was added 12 h after transfection. 48-72 h after transfection, the supernatant was collected and flash frozen. HeLa cells or K562 cells were transduced in the presence of 8 μg/mL polybrene (Sigma, H9268). After recovery, cells were directly used in experiments or optimized for expression by FACS.

Antibodies

The following antibodies were used in this study: ATF4 (1:1000), EIF2B3 (1:2000), EIF2B4 (11332–1-AP, 1:1000), EIF2α (1:1000), p-EIF2α (1:1000), α-GFP (1:1000), LC3B (1:1000), OMA1 (1:500), HRI/EIF2AK1 (1:3000), TIMM50 (1:2000), TOM20 (1:1000), PINK1 (1:1000), Phospho-Ubiquitin (Ser65) (1:1000), α-Puromycin (1:1000), α-TUB (1:2000), β-ACTIN (1:10000). Secondary antibodies used for immunoblotting were: goat anti-mouse IgG (H+L)-HRP (1:10000) and goat anti-rabbit IgG (H+L)-HRP (1:10000). Primary antibodies used for immunofluorescence were: p-EIF2α (1:100), TOM20 (1:100), HSP60 (1:1000), PEX14 (1:100), PARKIN (1:500), LC3B (1:50), α-GFP (1:100). Secondary antibodies used for immunofluorescence were donkey anti-mouse IgG AlexaFluor 488 (1:500), donkey anti-rabbit IgG AlexaFluor 555 (1:500), anti-goat IgG AlexaFluor 568 (1:500). Western blots were incubated with chemiluminescent substrate and detected using a Chemidoc imager (Bio-Rad Laboratories). Densitometry was used to quantify pEIF2α and TOM20 bands in the mitochondrial fraction with background correction. TOM20 levels were used for normalization.

Puromycylation assay

K562 cells were treated with requisite reagents such that there were ~500,000 cells/ml at the point of harvest. Puromycin (1 μM) was added 10 mins before harvest. Western blots were probed with anti-Puromycin antibody (1:1000) overnight at 4 °C.

Flow cytometry

Mitophagy in K562 or HeLa cells expressing mito-mKeima was quantified by flow cytometry. Cells were harvested, washed once with ice cold PBS, then resuspended in flow cytometry buffer (2.5 mg/ml fraction V BSA, 10 mM HEPES, 1 mM MgCl2, 50 μg/ml DNAse 1 in 1X HBSS (Thermo Fisher Scientific, 14175079) at pH 7.4) before analysis on a CytoFLEX S (Beckman Coulter). Flow cytometry data was analyzed in FlowJo v10.8 Software (BD Life Sciences). The mKeima acidic/neutral ratio was plotted, and the ratio threshold for mitophagy was set so that control cells had a baseline of 5% or less.

For quantifying mitophagy induced by expression of ubiquitin chains on the OMM, cells were transiently transfected with expression plasmids with Lipofectamine 3000. These cells were treated with DMSO or 100 nM BFA1 at 24 h after transfection. After 48 h, these cells were prepared for flow cytometry as detailed above. Data were collected from GFP/YFP positive cells. The mitophagy levels obtained were normalized by the corresponding BFA1-treated values.

qPCR

Total RNA was extracted from 1×10^6 cells using RNeasy mini kit (Qiagen, 74104). 200 ng of total RNA was used for cDNA synthesis by SuperScript III First-Strand Synthesis System for RT-PCR (Thermo Fisher Scientific, 18080-400) according to the manufacturer's protocol. Quantitative PCR amplification was done with primers for *DELE1* (Forward: 5' AGGCTGTGACTTCCATTCAG 3', Reverse: 5' TCGCCACTCTTCATGTTCTC 3') and *β-ACTIN* (Forward: 5' TCATCACCATTGGCAATGAG 3', 5' ACTTCATGATGGAGTTGAAG 3'), using Brilliant III Ultra-Fast SYBR® Green QPCR Master Mix (Agilent, 600882). Fold changes were calculated using the $\Delta\Delta C_t$ method.

Confocal microscopy and post-imaging processing

Confocal fluorescence images were acquired using an inverted Zeiss LSM 710 confocal microscope with a 63X Plan Apochromat objective. All images were processed using Fiji. All image modifications were performed on entire images and were performed identically between samples. Before analyzing the co-localization between TOM20 and p-EIF2α, the nuclear signal for p-EIF2α was

Please cite this article in press as: Chakrabarty et al., The HRI branch of the integrated stress response selectively triggers mitophagy, Molecular Cell (2024), https://doi.org/10.1016/j.molcel.2024.01.016

removed post-imaging using the DAPI channel. The Mander's coefficient algorithm in Fiji was run on at least 10 images per experiment, and 2-way ANOVA was used for statistical analysis from 4 independent experiments.

For quantifying the percentage of LC3B-GFP puncta colocalized with TOM20, ROIs containing cells expressing LC3B-GFP immunostained for GFP and TOM20 were selected randomly. Five images per experiment were randomly captured for each condition with a minimum of 2 cells per image ($n = 3$). To analyze the images Fiji and its plugins were used. We used the JACoP Fiji plugin for detecting colocalization based on the distance between the centroids of the spots.[48] Colocalization was normalized by the total number of LC3B-GFP particles. The particle analysis plugin from Fiji was used to determine the total number of LC3B-GFP puncta.

Sample preparation for immunofluorescence

For immunofluorescence, HeLa cells were seeded on multi-chambered coverglass bottomed dishes (Thermo Fisher Scientific, 154534). For HeLa cells expressing PARKIN, dishes were coated with poly-L-lysine. All cells were allowed to adhere for 24 h. Post treatment cells were briefly permeabilized with digitonin buffer (0.001% digitonin, 20 mM 4-(2-hydroxyethyl)-1-piperazineethanesulfonic acid [HEPES], 150 mM NaCl, 2 mM MgCl2, 2 mM EDTA, 320 mM sucrose, pH 7.4) for 2 mins at 37°C as described previously.[49] Digitonin-treated cells were fixed with 4% paraformaldehyde for 15 mins at 37°C. After fixation, cells were permeabilized with 0.1% Triton X100 in phosphate-buffered saline (PBS) at room temperature (RT). After blocking with 1% BSA in PBS for 30 mins at RT, cells were incubated with primary antibodies for 2 h at RT. After 4 washes of 5 mins each with PBS, cells were stained with AlexaFluor-555 (or 488) coupled secondary antibody for 1 h at RT and then washed with PBS. Slides were mounted with Fluoro-Gel (Electron Microscopy Sciences, 17985). For HSP60 immunostaining, PARKIN and GFP immunostaining, the same protocol was used, except that the digitonin permeabilization step was omitted. In case of LC3B immunofluorescence, fixation with 4% paraformaldehyde for 10 min at room temperature was followed by permeabilization with 50 μg/ml digitonin for 5 min.

Rapalog-induced FRB-FKBP dimerization assay

The FRB-FKBP system as described previously[46] was adapted to achieve mitochondrial or peroxisomal recruitment of EIF2α^{WT}, EIF2α^{S51A} and EIF2α^{S51D}. 2XFKBP was fused to GFP and HA tagged EIF2α^{WT}, EIF2α^{S51A} and EIF2α^{S51D} in the pHAGE lentiviral vector. For mitochondrial or peroxisomal recruitment assays, cells were treated with 500 nM rapalog for 24 h. Cells were analyzed by flow cytometry or immunostaining.

CRISPRi screen

The genome-wide CRISPRi screen was performed in duplicate as described previously.[9,10] The hCRISPRi-v2 library targeting 18,905 genes (5 sgRNAs per gene,) was transduced into 400 million K562-CRISPRi-mito-mKeima cells at a multiplicity of infection (MOI) < 1. This MOI corresponds to 25-30% BFP-positive cells at 48 h post infection. Cells were grown in 0.5-1 L of media in 1 L spinner flasks. 48 h after spin-infection with the genome-wide library, sgRNA-positive cells were selected with 1 μg/mL puromycin for three days. Cells were fed with fresh media containing puromycin every 24 h. Post selection, cells were allowed to recover for two days, treated with 1 mM DFP for 24 h, and sorted on a BD FACS Aria Fusion Cell Sorter. During sorting, cells were stained with SYTOX Green (Thermo Fisher Scientific, S34860) to remove any dead cells and gated for BFP, as well as for the acidic and neutral mito-mKeima signal. Cells were sorted based on the acidic/neutral ratio of this final gated population. 25 million cells with either the highest (25%) or lowest (25%) acidic/neutral ratio were collected, pelleted, and flash frozen. An unsorted cell population with similar cell numbers was also pelleted and flash frozen. Genomic DNA was purified using the Nucleospin Blood XL kit and amplified by index PCR with barcoded primers. The resulting guide library (~264 bp) was purified using SPRIselect beads (Beckman Coulter, B23318). After quality check of the purified DNA, sequencing was performed with an Illumina HiSeq2500 high throughput sequencer. Sequencing reads were aligned to the CRISPRi-v2 library sequences, counted, and quantified.[9] Generation of negative control genes and calculation of phenotype scores and Mann-Whitney p values were performed as described previously.[9,10] Gene-level phenotypes, p values, and counts are available in Table S1.

Subcellular fractionation

Mitochondrial isolation from K562 and HeLa cells was adapted from an established protocol.[50] After centrifuging cells at 300 *g* for 5 mins, the cell pellet was washed once in mitochondria isolation buffer (MIB: 210 mM mannitol, 70 mM sucrose, 5 mM HEPES pH 7.4, 10 mM EDTA) after addition of 1X HALT protease inhibitor cocktail (Thermo Scientific, 78439). The pellet was resuspended in MIB and incubated on ice for 10 minutes. Cells were then lysed with a glass Dounce homogenizer with a tight-fitting pestle for 50 strokes. An aliquot was removed for protein quantification to normalize samples. The cell lysate was pelleted at 1000 *g* for 5 minutes to remove nuclei and unbroken cells, and then the supernatant was transferred to a clean tube. This step was repeated twice. Nuclei-free cell lysate was then centrifuged at 10,000 *g* for 10 minutes. The supernatant was removed to a separate tube and the mitochondria-containing pellet (Mito) was washed once in MIB and resuspended in a small volume (50-100 μl) of isolation buffer. To generate the crude cytosolic fraction (Cyto), supernatant from the previous step was centrifuged at 20,000 *g* for 30 mins. To isolate the ER enriched fraction, the post-10,000 *g* supernatant was centrifuged at 100,000 *g*, and the pellet was resuspended in isolation buffer. The supernatant thus obtained was a clarified cytosolic fraction (Cyto-II). To normalize mitochondrial samples, the protein concentration was measured using the DC Protein assay (BioRad).

Please cite this article in press as: Chakrabarty et al., The HRI branch of the integrated stress response selectively triggers mitophagy, Molecular Cell (2024), https://doi.org/10.1016/j.molcel.2024.01.016

QUANTIFICATION AND STATISTICAL ANALYSIS

Pairwise comparisons were made using the Student's t-test. All data are represented as mean ± s.d. ****, $p \leq 0.0001$; ***, $p \leq 0.001$; **, $p \leq 0.01$; *, $p \leq 0.05$; ns, $p \geq 0.05$. For the experiments involving colocalization, 2-way ANOVA was used for statistical analysis from a minimum of 3 independent experiments.

ADDITIONAL RESOURCES

No additional resources were generated by this study.